

# Numerical Simulation of Split-Hopkinson Pressure Bar Test on High-Density Polyethylene

Shou Chen

Army Logistics University of PLA, Dept. of Military Facilities, Chongqing 401331, China  
 649741539@qq.com

This paper attempts to provide new insights into the engineering application of high-density polyethylene (HDPE) under impact load and the development of HDPE materials. For this purpose, an ANSYS/LS-DYNA numerical simulation was carried out for split-Hopkinson pressure bar (SHPB) impact compression test. A total of six working conditions (WCs) were arranged for the simulation. Comparing the stress waveforms of different specimens at the same impact velocity, it is concluded that the HDPE material has a certain energy dissipation effect under the impact load, but the effect cannot be effectively enhanced with the addition of HDPE sheets. The author also investigated the HDPE mechanical properties at different impact velocities of the bullet. The results show that the mechanical properties of HDPE material have a certain strain rate dependency under the impact load; the deformation of HDPE sheet became increasingly serious with the increase of the impact velocity of the bullet.

## 1. Introduction

High-density polyethylene (HDPE) has been extensively used thanks to its high strength, good toughness, excellent electrical insulation, and ease of processing (Yang et al., 2016). In recent years, much research has been done on the mechanical properties of HDPE at home and abroad. Below are some of the representative studies.

Using the Sherwood-Frost's constitutive model (Xu et al., 2016), Marcel et al. (Sherwood and Frost, 1992) investigated the mechanical properties of HDPE through a uniaxial tensile test, and discovered the positive correlation between the mechanical properties and the strain rate. Chen Zipeng et al. conducted a sheet tension test to disclose the effects of the strip pattern, tensile rate and tensile direction on the tensile mechanical properties of HDPE. The test results show that all three factors have an impact on the failure mode of HDPE sheet, and that the maximum tensile stress of HDPE clearly depends on the strain rate. Li Junwei et al. (Li and Huang, 2008) experimentally explored the relationship between the mechanical parameters (e.g. Poisson's ratio, tensile modulus, maximum tensile stress, and tensile strain) of HDPE sheet and the tensile strain rate, and developed the stress-strain relationship model considering the strain rate dependency of HDPE sheet. Mills et al. (Mills and Masso, 2005) pointed out the isotropy of the mechanical properties of HDPE. After fitting and analysing the data of multiple tests, Hutchinson et al. (Neale and Hutchinson, 1983) proposed a constitutive equation for the constitutive relation of polymers at a constant tensile rate. On this basis, Kwon et al. (Kwon and Jar, 2008) obtained a constitutive equation with a wider applicable range through tests and numerical simulations. The equation overcomes the non-convergence of the calculation results in numerical simulation of heavily deformed HDPE. It applies to the numerical simulation of most HDPE uniaxial tensile tests.

The widening of applicable range has complicated the service environment of HDPE. In many fields, HDPE materials must withstand high-speed loads, in addition to static or low-speed loads. For instance, the HDPE-based flexible protective structure needs to resist the penetration effect of high-speed shells and the blast effect of explosives. Under high-speed loads, HDPE materials will deform at a strain rate several orders of magnitude higher than that of static or low-speed loads, and exhibit completely different mechanical properties. Nevertheless, there is few report on HDPE mechanical properties at high strain rate.

The split-Hopkinson pressure bar (SHPB) impact compression test is one of the technologies that can provide high-strain-rate loading. Capable of creating a strain rate in  $10^1 \text{ s}^{-1} \sim 10^2 \text{ s}^{-1}$  (Lu, 2013), this technology is suitable for the study of impact compression properties of materials. Considering these, this paper explores the HDPE mechanical properties under impact load through numerical simulation of SHPB test, aiming to gain new insights into the engineering application of HDPE under impact load and the development of HDPE materials.

## 2. Selection of Material Models and Parameters

### 2.1 Material model for bars

The bullet, incident bar and transmission bar were all simulated by \*MAT\_ELASTIC, Material Type 1 in LS-DYNA. This is an isotropic elastic material and is available for beam, shell and solid elements. The parameters of the model are density  $\rho=7.85 \text{ g/cm}^3$ , elastic modulus  $E=2.1 \times 10^5 \text{ MPa}$  and Poisson's ratio  $\nu=0.25$ .

### 2.2 Material model for concrete

The concrete was simulated by \*MAT\_JOHNSON\_HOLMQUIST\_CONCRETE (HJC), Material Type 111 in LS-DYNA. Proposed by Holmquist et al. (Johnson and Holmquist, 2011), the HJC is a dynamic constitutive model that can accurately simulate concrete subjected to large strains, high strain rates and high pressures. There are 21 parameters in the HJC, including density  $\rho_0$ , compressive strength  $f_c$ , strain rate  $\epsilon_0$ , failure type  $F_s$ , six strength parameters (G, A, B, C, N and  $S_{max}$ ), three damage parameters ( $\epsilon_{fmin}$ , D1 and D2), and eight pressure parameters (T,  $P_c$ ,  $\mu_c$ ,  $P_l$ ,  $\mu_l$ , K1, K2 and K3). The specific value of each parameter was obtained from Reference. The keyword \*MAT\_ADD\_EROSION was included into the material model to define the failure criteria.

Table 1: Parameters for projectile material

$\rho_0/(\text{kg/m}^3)$	G/GPa	A	B	C	N	$f_c/\text{GPa}$
2440	14.86	0.79	1.60	0.007	0.61	0.048
T/GPa	$\epsilon_0/(\times 10^{-6})$	$\epsilon_{fmin}$	$S_{max}$	$P_c/\text{GPa}$	$\mu_c$	$P_l/\text{GPa}$
0.004	1	0.01	7.00	0.016	0.001	0.80
$\mu_l$	D1	D2	K1/GPa	K2/GPa	K3/GPa	$F_s$
0.10	0.04	1.00	85	-171	208	0.004

### 2.3 Material model for HDPE

The HDPE was simulated by \*MAT\_PLASTICITY\_POLYMER, Material Type 89 in LS-DYNA. This is an elastic-plastic material model that can define an arbitrary stress-strain curve and arbitrary strain rate dependency. It is intended for applications where the elastic and plastic sections of the response are not clearly distinguishable. Besides, the model can simulate the exact brittle response of the polymer at high strain rates. The parameters of the model are density  $\rho=0.942 \text{ g/cm}^3$ , elastic modulus  $E=1,034.2 \text{ MPa}$  and Poisson's ratio  $\nu=0.45$ .

In the model, the stress-strain curve is illustrated by the Kwon constitutive equation for heavily deformed HDPE at high strain rate (Kwon and Jar, 2007). The equation can be expressed as:

$$\sigma(\epsilon) = \begin{cases} \frac{3}{2(1+\nu)} E \epsilon & \epsilon \leq \epsilon_y \\ d \{ [a(\epsilon+b)]^{(c-1)} - [a(\epsilon+b)^{-c}] \} + e & \epsilon_y < \epsilon \leq \epsilon_n \\ \alpha k \epsilon^N & \epsilon_n < \epsilon \leq \epsilon_t \\ K \exp(M \epsilon^\beta) & \epsilon > \epsilon_t \end{cases}$$

It is a piecewise function and solve the problem on the calculation results of the numerical simulation doing not converge. The values of elastic modulus E and Poisson's ratio  $\nu$  were determined by the experimental data. The values of the other parameters were defined by the user. The specific value of each parameter was determined according to Reference.

Table 2: Parameter values of Kwon constitutive equation

$\epsilon_y$	d	a	b	c	e
0.015	-22.29	33.41	0.0149	0.001	15.50
$\alpha k$	N	$\epsilon t$	K	M	$\beta$
35.517	0.077	0.32	30.66	0.4953	1.80

### 3. Construction of Finite Element Model

The finite element model was established according to the actual size (Figure 1). Specifically, the bullet is 800 mm long and 37 mm in diameter; the 3,200 mm long incident bar is a variable section steel bar whose variable section is 450 mm long, incident end diameter is 37 mm and straight section diameter is 74 mm; the transmission bar is 1,600 mm long and 74 mm in diameter; the concrete specimen is 30 mm thick and 60 mm in diameter; the HDPE sheet is 2 mm thick and 60 mm in diameter.

The bullet, incident bar, transmission bar and concrete were meshed into solid elements SOLID164, while the HDPE was meshed into shell elements SHELL163. The surface-to-surface contacts between the bullet and the incident bar, the incident bar and the specimen, and the specimen and the transmission bar were defined as \*CONTACT\_AUTOMATIC\_SURFACE\_TO\_SURFACE.

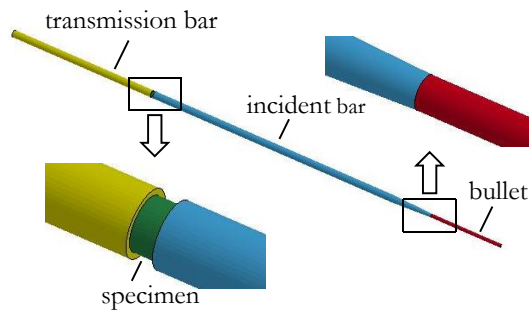


Figure 1: Finite element model

In the SHPB test, the impact velocity of the bullet was controlled by adjusting the pressure released by the loading device. The pressure is positively correlated with the impact velocity of the bullet and the strain rate of the specimen. During the simulation, the initial velocity of the bullet was controlled to simulate different pressures. Three impact velocities of the bullet were simulated: 5 m/s, 10 m/s and 15 m/s. There are three types of specimens: (a) pure concrete; (b) concrete embedded with one HDPE sheet; (c) concrete embedded with two HDPE sheets (Figure 2). A total of six working conditions (WCs) were configured to disclose the mechanical properties of HDPE under impact load (Table 3). The simulation of blank test is denoted as WC1.

Table 3: WCs

WC	Impact velocity of bullet/(m/s)	Type of specimen
1	15	no sheet
2	15	a
3	15	b
4	15	c
5	10	b
6	5	b

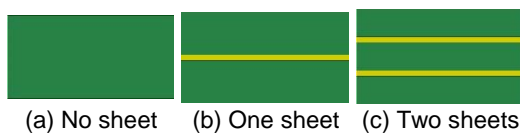


Figure 2: Types of specimens

## 4. Analysis of Mechanical Properties

### 4.1 Effect of the number of sheets

The stress waveforms were obtained in WCs 1, 2, 3 and 4 at the same impact velocity of the bullet. According to the positions of strain gauges in the SHPB test, two elements were selected from the incident bar and the transmission bar for numerical simulation. The strain-time curves of the two elements were plotted, forming the numerically simulated waveforms (Figure 3).

As shown in Figure 3, the waveforms of WCs 2, 3 and 4 are basically the same. Under the action of the loading device, the bullet hit the incident bar at a certain initial velocity. The stress wave generated in the incident bar at the moment of impact is called the incident wave. The incident wave propagated along the transmission bar to the specimen, leading to deformation and even failure of the specimen. The incident wave was partially dissipated, partially reflected to the incident bar (reflected wave), and partially transmitted through the specimen to the transmission bar, creating a stress wave in that bar (transmitted wave). Specifically, the area under the curve (AUC) of the incident wave reflects the total impact energy generated at the moment of collision between the bullet and the incident bar, while the AUC of the reflected wave and the transmitted wave represents the residual impact energy. The difference between the total impact energy and the residual impact energy equals the amount of dissipated impact energy, most of which occurred during specimen deformation and destruction.

As mentioned above, WC1 is the simulation of blank test designed to yield the original waveform, a reference for the waveforms in the other WCs. The peak strain of the transmitted wave was  $7.78 \times 10^{-4}$  in WC1, which is 55.40 % higher than that in WC2 ( $3.47 \times 10^{-4}$ ), 64.52 % higher than that in WC3 ( $2.76 \times 10^{-4}$ ) and 70.05 % higher than that in WC4 ( $2.33 \times 10^{-4}$ ). In WCs 2-4, the specimen is respectively pure concrete, concrete embedded with one HDPE sheet, and concrete embedded with two HDPE sheets. Through the comparison between the four WCs, it is clear that the HDPE material consumed a certain amount of energy under the impact load; however, the specimen did not consume a significantly greater amount of energy with the increase in the number of HDPE sheets, indicating that concrete is the main energy consumer in our simulation. Similar conclusion was obtained through the simulation of other WCs. The results of the other WCs are not provided due to the limited space.

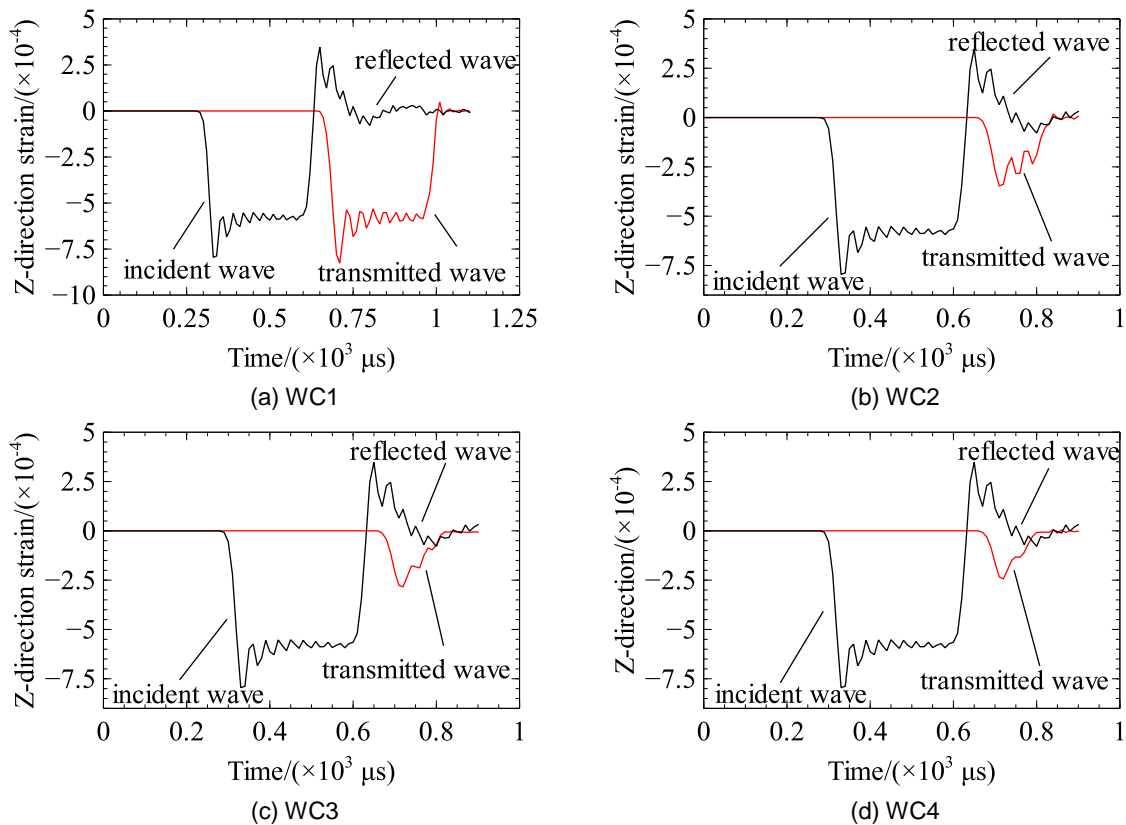


Figure 3: Waveforms in different WCs

#### 4.2 Effect of the impact velocity of the bullet

Specimen (a) (concrete embedded with one HDPE sheet) was selected for simulation at the WCs whose impact velocities of the bullet are 5 m/s, 10 m/s and 15 m/s, respectively. The stress-time curves of the HDPE sheet along the bar were plotted (Figure 4).

It can be seen from Figure 4 that the stress on the HDPE sheet remained at zero before the stress wave reaching the specimen; the stress soared rapidly towards the peak value once the stress wave arrived at the

specimen via the incident bar. Then, the stress on the HDPE sheet gradually declined to zero, as the incident wave was partially dissipated, partially reflected to the incident bar, and partially transmitted to the transmission rod.

In WC6, the peak stress of the HDPE sheet was 48.70 MPa when the impact velocity of the bullet was 5 m/s. In WC5, the peak stress was 56.00 MPa, 14.99 % higher than that in WC6, when the impact velocity of the bullet was 10 m/s. In WC3, the peak stress was 60.48 MPa when the impact velocity of the bullet was 15 m/s; the stress value is 24.19 % higher than that in WC6 and 8 % higher than that in WC5. As mentioned before, the impact velocity of the bullet is positively correlated with the pressure released by the loading device and the strain rate of the specimen. Therefore, the mechanical properties of HDPE material have a certain strain rate dependency under the impact load, i.e. the peak stress increases with the strain rate.

In future, the impact of strain rate on HDPE material will be further examined. A possible way is to reconstruct the strain-time curves of HDPE sheets into the stress-strain curves under the impact load via the two-wave method (Yin et al., 2007).

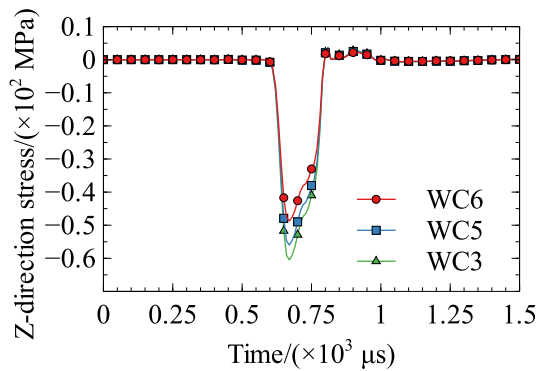


Figure 4: Stress-time curves in different WCs

### 4.3 Analysis of failure mode

Figure 5 shows the failure pattern of HDPE sheet in WC4. It can be seen that the HDPE was deformed more severely in the peripherals than in the central part. This means the peripherals of the HDPE sheet absorbed more impact energy than the central part during the impact compression test. Moreover, the sheet deformation was more severe on the side near the incident bar than the side away from that bar, indicating that the amount of absorbed impact energy is positively correlated with the closeness to the incident bar. This is an indirect evidence for the conclusion that the energy consumption of the specimen cannot be effectively enhanced with the addition of HDPE sheets.

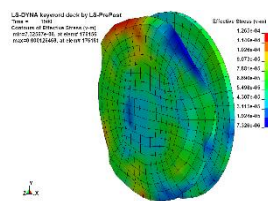


Figure 5: Failure pattern in WC4

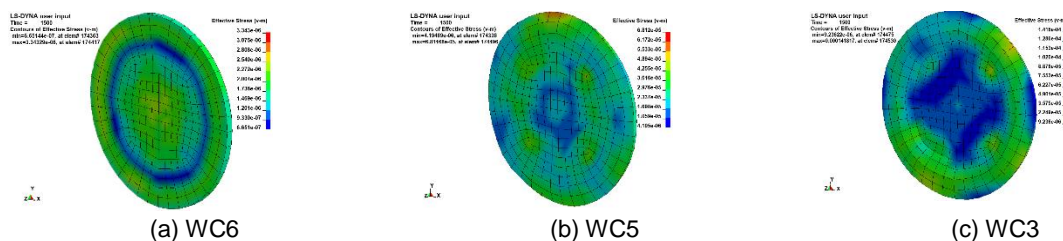


Figure 6: Failure modes in different WCs

According to the failure modes in WCs 3, 5 and 6 (Figure 6), the failure mode of the HDPE sheet varied with the impact velocity of the bullet. In general, the strain rate and the degree of deformation both increased with the impact velocity.

When the impact velocity of the bullet was 5 m/s, there was only a few cracks in the concrete with no reduction in the number of grids; the embedded HDPE sheet was free from any deformation or failure. When the impact velocity of the bullet is 10 m/s, the number of concrete grids decreased in the peripherals of the specimen, and the concrete suffered from surface failures. In this case, the plastic deformation appeared at the outermost periphery of the embedded HDPE sheet. When the impact velocity of the bullet increased to 15 m/s, cracks emerged simultaneously across the concrete, the entire concrete was severely damaged except for the core area, and many grids went missing. Similarly, the embedded HDPE sheet was severely damaged by severe plastic deformation except for the central part. The numerical simulation will be verified with experiments.

## 5. Conclusion

(1) Comparing the stress waveforms of different specimens at the same impact velocity, it is concluded that the HDPE material has a certain energy dissipation effect under the impact load, and the specimen with two sheets is more energy-efficient. However, the effect cannot be effectively enhanced with the addition of HDPE sheets.

(2) The comparison of HDPE mechanical properties at different impact velocities show that the mechanical properties of HDPE material have a certain strain rate dependency under the impact load, i.e. the peak stress increases with the strain rate. In future research, the impact of strain rate on mechanical properties should be further investigated by reconstructing the stress-strain curves of HDPE material.

(3) The HDPE failure modes in different WCs were compared, revealing that the sheet closer to the incident bar was more seriously deformed, and the peripheral deformation was greater than the central deformation in the same sheet during the impact compression test. Furthermore, the deformation of HDPE sheet became increasingly serious with the increase of the impact velocity of the bullet. The numerical simulation will be verified with experiments.

## Reference

- Johnson G.R.A., Holmquist T.J., 2011, Computational Constitutive Model for Glass Subjected to Large Strains, High Strain Rates and High Pressures, *Journal of Applied Mechanics*, 78, 051003.
- Kwon H.J., Jar P.Y.B., 2007, Application of Essential Work of Fracture Concept to Toughness Characterization of High-Density Polyethylene, *Polymer Engineering & Science*, 47, 1327–1337.
- Kwon H.J., Jar P.Y.B., 2008, On the Application of FEM to Deformation of High-Density Polyethylene, *International Journal of Solids and Structures*, 45, 3521–3543.
- Li J.W., Huang H.W., 2008, Study on Tensile Strain Rate Correlation of Geocell HDPE Sheet, *Journal of Building Materials*, 11, 47-51.
- Lu F.Y., 2013, son's Pole Experimental Technique, Science Press, Beijing.
- Mills N.J., Masso M.Y., 2005, Finite Element Analysis (FEA) Applied to Polyethylene Foam Cushions in Package Drop Tests, *Packaging Technology & Science*, 18, 29–38.
- Neale K.W., Hutchinson J.W., 1983, Neck Propagation, *Journal of the Mechanics & Physics of Solids*, 31, 405-426, DOI: 10.1016/0022-5096(83)90007-8
- Sherwood J.A., Frost C.C., 1992, Constitutive Modeling and Simulation of Energy Absorbing Polyurethane Foam under Impact Loading, *Polymer Engineering & Science*, 32, 1138–1146, <https://doi.org/10.1002/pen.760321611>
- Xu J.S., Tong X., Ma S.E., 2016, Study on Uniaxial Tensile Properties and Constitutive Relationship of High Density Polyethylene, *China Plastics*, 30, 88-92.
- Yang X.M., Wang W., Tian W., 2016, Properties of Nano MgO/High Density Polyethylene Composites, *Composite Materials*, 33, 234-239.
- Yin L.Y., Xing N., Lan X.F., 2007, A Brief History of Steroid Therapy for Guillain-Barré Syndrome, *NeuroQuantology*, 15, 153–157.